EDGE ARTICLE

Check for updates

High-affinity 1:2 recognition based on naphthyl-azocalix[4]arene and its application as a cleavable noncovalent connector in constructing responsive supramolecular polymeric materials†

Shun-Yu Yao,‡[a] An-Kang Ying,‡[a] Wen-Chao Geng,[a] Fang-Yuan Chen,[a] Xin-Yue Hu, [ID][a] Kang Cai [ID] *[b] and Dong-Sheng Guo [ID] *[ac]

Macrocyclic hosts which can bind two guests simultaneously with high affinity, such as cucurbit[8]uril, are highly useful for a wide range of applications by acting as noncovalent connectors. However, the integration of stimuli-controlled release properties into such robust noncovalent connectors would be even more desirable. Here, we introduce Naph-SAC4A, a naphthyl-extended deep-cavity azocalix[4]arene with hypoxia-responsiveness, which exhibits exceptional 1:2 hosting abilities for organic dyes in aqueous solution with affinities ranging from 10^{14} to 10^{16} M^{-2}. Furthermore, Naph-SAC4A was employed as a robust hypoxia-cleavable noncovalent connector to construct linear supramolecular polymers and crosslinked supramolecular hydrogels. Both structures exhibit responsiveness to hypoxic stimuli. With its high-affinity 1:2 recognition, unique hypoxia-responsiveness, and easy accessibility, Naph-SAC4A holds great potential for smart supramolecular polymeric materials.

Introduction

Macrocyclic hosts are key players in supramolecular chemistry, with materials based on their recognition properties being widely utilized in fields such as biomedicine,[1–6] nanotechnology,[7–10] and smart soft materials.[11–15] Most macrocyclic hosts typically form 1:1 host–guest complexes, a fundamental and widely studied binding mode.[16–19] While these hosts are well-explored, those capable of accommodating two guest molecules simultaneously are much rarer. This is due to the increased entropy penalty associated with three-component binding and the higher structural and size-matching requirements for both the host and guests.[20–23] Macrocyclic hosts capable of 1:2 host–guest binding are particularly valuable in supramolecular chemistry. Acting as non-covalent connectors or "molecular glues", they can bridge two molecular units

within a confined nanospace, facilitating applications in sensing, supramolecular catalysis, noncovalent molecular conjugation, and supramolecular polymerization. Such macrocyclic hosts which can engage in 1:2 host–guest binding are highly valuable because they can function as non-covalent connectors or "molecular glues", linking two molecular motifs together. Notable examples of such hosts include γ-cyclodextrin
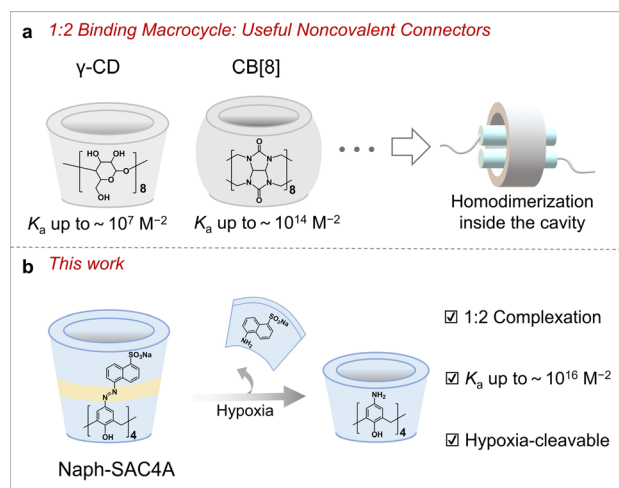
[a]*College of Chemistry, State Key Laboratory of Elemento-Organic Chemistry, Key Laboratory of Functional Polymer Materials (Ministry of Education), Frontiers Science Center for New Organic Matter, Collaborative Innovation Center of Chemical Science and Engineering, Nankai University, 300071 Tianjin, China. E-mail: dshguo@nankai.edu.cn*

[b]*College of Chemistry, Nankai University, Tianjin, 300071, China. E-mail: kangcai@nankai.edu.cn*

[c]*Xinjiang Key Laboratory of Novel Functional Materials Chemistry, College of Chemistry and Environmental Sciences, Kashi University, Kashi 844000, China*

† Electronic supplementary information (ESI) available. See DOI: https://doi.org/10.1039/d5sc00075k

‡ These authors contributed equally: Shun-Yu Yao and An-Kang Ying.

Scheme 1 (a) Two typical 1:2 binding macrocycles, γ-CD and CB[8], which exhibit binding strength up to 10^7 and 10^{14} M^{-2}, respectively. (b) Naph-SAC4A as a new 1:2 binding host with not only high binding affinity (up to 10^{16} M^{-2}) but also inherent hypoxia-responsiveness.

(γ-CD)[24–26] and cucurbit[8]uril (CB[8])[27–31] (Scheme 1), which utilize hydrophobic interactions within their cavities to bind small, elongated guest molecules. However, γ-CD typically forms 1 : 2 host–guest complexes with relatively low binding constants ($<10^8$ M^{-2}), hindering its use in high-concentration systems.[32–34] In contrast, CB[8] can form 1 : 2 host–guest complexes with extraordinarily high binding constants, reaching up to 10^{14} M^{-2}, making it a highly robust non-covalent connector.[35,36] This remarkable affinity grants CB[8] unparalleled advantages in the construction of supramolecular polymers, hydrogels, and framework materials.[37–39] Despite these advantages, the poor solubility and high synthesis cost of CB[8] pose significant challenges, limiting its widespread application.[40,41] Additionally, the 1 : 2 host–guest complexes of CB[8] typically require specific stimuli-responsive guest molecules (such as azobenzene or spirocyclic derivatives) to enable controlled release, which limits its use in designing responsive materials.[42–45] Therefore, there is a strong demand for the development of novel macrocyclic hosts with exceptional 1 : 2 guest binding abilities and greater versatility for advancing stimulus-responsive supramolecular materials.

Our group previously reported a naphthalenesulfonic acid-modified azobenzene calix[4]arene (Naph-SAC4A, Scheme 1) with deep hydrophobic cavities that enable ultrahigh 1 : 1 binding affinities (up to 10^{13} M^{-1}) towards a range of clinical drugs and fluorescent dyes in aqueous solutions.[46–48] The unique property of Naph-SAC4A lies in its ability to undergo azo group cleavage under hypoxic conditions, facilitating controlled guest release.[49–52] Given that Naph-SAC4A features a cone-shaped hydrophobic cavity similar to γ-CD, we hypothesized that it could potentially form 1 : 2 host–guest complexes, with the deep hydrophobic cavity providing a strong binding affinity.[53] Moreover, its inherent hypoxia-triggered release property sets it apart from γ-CD and CB[8], as it can serve as a controllable non-covalent connector, a feature particularly advantageous for constructing stimulus-responsive supramolecular materials.[54–58] Furthermore, Naph-SAC4A is easy to synthesize in a single step and exhibits excellent water solubility, which significantly broadens its practical applicability.

Given the structural diversity of fluorescent dyes and their widespread use in biomedical imaging and related fields, we systematically explored the host–guest recognition between Naph-SAC4A and a series of organic dye molecules to uncover unique binding characteristics and potential applications. Our results confirm that Naph-SAC4A can indeed form stable 1 : 2 host–guest complexes with binding affinities ranging from 10^{14} M^{-2} to 10^{16} M^{-2}, even surpassing CB[8] in binding strength. To further demonstrate the advantages of Naph-SAC4A in supramolecular polymer formation, especially in designing stimulus-responsive supramolecular materials, we synthesized a dimeric guest (D-Cy5) of cyanine 5 (Cy5) and Cy5-modified hyaluronic acid (HA-Cy5). Mixing these with Naph-SAC4A successfully resulted in the formation of linear supramolecular polymers and cross-linked networks, which also exhibited hypoxia-responsive behavior.

Results and discussion

Preparation of Naph-SAC4A and host–guest titrations

Building on our previous work,[59] we successfully synthesized Naph-SAC4A via a one-step coupling reaction between 5-diazonium-1-naphthalenesulfonic acid and calix[4]arene (C4A), yielding Naph-SAC4A in 59% yield, followed by a simple recrystallization process. In this study, the counterion of Naph-SAC4A is sodium ion (Na$^+$), and the ease of synthesis is a notable advantage of this molecule. Our prior studies revealed that Naph-SAC4A exhibits high affinity for a range of hydrophobic guests (e.g., rocuronium bromide and tetraarylporphyrins) with relatively large molecular sizes, forming stable 1 : 1 host–guest complexes.[60,61] Given that Naph-SAC4A possesses a relatively large hydrophobic cavity, we hypothesized that it might similarly accommodate two elongated, planar guest molecules, analogous to the binding mode of γ-CD and CB[8].[62–64]

To investigate this hypothesis, we selected trans-4-(4-(dimethylamino) styryl)-1-methylpyridine (ASP) as a model guest to study the 1 : 2 host–guest recognition property of Naph-SAC4A in PBS solution (Fig. 1a). Notably, as encountered in previous studies of other azocalixarene derivatives,[65,66] attempts to investigate the binding process in aqueous solution using ITC were unsuccessful. This is likely due to the amphiphilic nature of Naph-SAC4A, with four negative charges that, upon binding with a positively charged guest, lead to reduction in overall negative charge and further aggregation that complicates the thermodynamic analysis. Given that ASP is a fluorescent dye, we employed fluorometric titrations to examine the binding process of ASP with Naph-SAC4A (Fig. 1b). A Job's plot analysis revealed a clear inflection point at an [ASP]/[ASP + Naph-SAC4A] ratio of approximately 66%, suggesting a 2 : 1 host–guest binding stoichiometry (Fig. 1c). Upon titrating Naph-SAC4A into an ASP solution, we observed a gradual quenching of ASP's fluorescence. The fluorometric titration curve also displayed a clear turning point at 0.50 equivalents of Naph-SAC4A, further supporting the formation of a 1 : 2 host–guest complex. Data fitting to a 1 : 2 binding model provided the binding constants $K_1 = (2.33 \pm 1.08) \times 10^7$ M^{-1} and $K_2 = (8.57 \pm 1.06) \times 10^6$ M^{-1}, respectively. These high binding affinities are relatively rare, even for the 1 : 2 ternary complexes of CB[8].

Encouraged by this result, we extended our investigation to evaluate the binding mode and affinities of Naph-SAC4A with 15 common fluorescent dyes (Fig. 2 and S8–S23†) frequently used in biological imaging (Fig. 2). The guest dyes selected included neutral red (NR), brilliant cresyl blue (BCB), MB, acridine yellow (ADY), ASP, 6MNEP, astrazon pink FG (AP-FG), astrazon red 6B (AR-6B), cyanine 3-dimethyl (Cy3-DM), cyanine 5-dimethyl (Cy5-DM), IR676 iodide (IR676), cyanine 5-monocarboxy (Cy5-MC), IR775 chloride (IR775), IR780 iodide (IR780), N-ethylamino-4-azacyclobutyl-1,8-naphthalimide (EANA), and 1-pyrenemethanamine hydrochloride (Pya). The host–guest binding constants for these guests are shown in Table 1. Similar to ASP, fluorometric titrations and Job's plot analyses demonstrated that all the 15 dyes formed 1 : 2 host–guest complexes with Naph-SAC4A. The titration curves revealed high binding affinities,
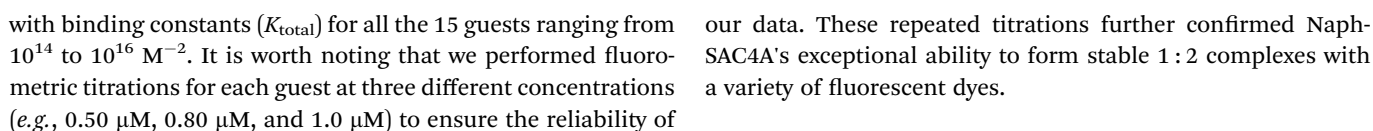
Fig. 1 (a) Chemical formulae of Naph-SAC4A and ASP. (b) Fluorometric titration curves obtained by tracking the fluorescence intensity at λ_{em} = 608 nm and fitted according to the 1:2 direct binding stoichiometry. Inset: fluorometric titration spectra obtained by gradually adding Naph-SAC4A (up to 1.19 µM) to ASP (0.50 µM) in PBS solution (10 mM, pH = 7.4) at 25 °C, λ_{ex} = 450 nm. (c) The Job's plot obtained by tracking the variation in the fluorescence emission at 608 nm for different ratios of Naph-SAC4A and ASP at a fixed total concentration of 1.0 µM.

with binding constants (K_{total}) for all the 15 guests ranging from 10^{14} to 10^{16} M^{-2}. It is worth noting that we performed fluorometric titrations for each guest at three different concentrations (e.g., 0.50 µM, 0.80 µM, and 1.0 µM) to ensure the reliability of our data. These repeated titrations further confirmed Naph-SAC4A's exceptional ability to form stable 1:2 complexes with a variety of fluorescent dyes.

Fig. 2 Chemical formulae of guest dyes and their abbreviations.

Table 1 Stepwise K_1 and K_2, overall K_{total}[a] association constants,[b] and interaction factors α,[c] for the complexation of Naph-SAC4A toward guests

Guests	K_1 (M^{-1})	K_2 (M^{-1})	K_{total} (M^{-2})	α
NR	$(5.91 \pm 0.71) \times 10^7$	$(1.47 \pm 0.36) \times 10^8$	$(8.83 \pm 3.21) \times 10^{15}$	9.9
BCB	$(6.92 \pm 1.70) \times 10^7$	$(1.24 \pm 0.25) \times 10^8$	$(8.29 \pm 0.57) \times 10^{15}$	7.2
MB	$(8.57 \pm 0.66) \times 10^7$	$(2.51 \pm 0.89) \times 10^8$	$(2.12 \pm 0.63) \times 10^{16}$	11.7
ADY-G	$(8.05 \pm 0.60) \times 10^7$	$(2.82 \pm 0.68) \times 10^8$	$(2.30 \pm 0.71) \times 10^{16}$	14.1
ASP	$(2.33 \pm 1.08) \times 10^7$	$(8.57 \pm 1.06) \times 10^6$	$(1.93 \pm 0.64) \times 10^{14}$	1.5
6MNEP	$(7.14 \pm 0.44) \times 10^7$	$(2.86 \pm 0.54) \times 10^7$	$(2.05 \pm 0.47) \times 10^{15}$	1.6
AP-FG	$(8.43 \pm 0.51) \times 10^7$	$(2.40 \pm 0.96) \times 10^8$	$(1.99 \pm 0.73) \times 10^{16}$	11.4
AR-6B	$(7.65 \pm 1.11) \times 10^7$	$(1.71 \pm 0.45) \times 10^8$	$(1.32 \pm 0.43) \times 10^{16}$	9.0
Cy3-DM	$(8.03 \pm 0.79) \times 10^7$	$(3.17 \pm 0.52) \times 10^8$	$(2.57 \pm 0.67) \times 10^{16}$	15.8
Cy5-DM	$(1.40 \pm 0.41) \times 10^8$	$(2.98 \pm 0.41) \times 10^8$	$(4.21 \pm 1.62) \times 10^{16}$	8.5
IR-676	$(1.48 \pm 0.39) \times 10^8$	$(3.07 \pm 0.48) \times 10^8$	$(4.47 \pm 1.05) \times 10^{16}$	8.3
Cy5-MC	$(8.76 \pm 0.81) \times 10^7$	$(1.68 \pm 0.17) \times 10^8$	$(1.48 \pm 0.24) \times 10^{16}$	7.7
IR-775	$(9.80 \pm 0.79) \times 10^7$	$(2.61 \pm 0.51) \times 10^8$	$(2.59 \pm 0.43) \times 10^{16}$	10.7
IR-780	$(1.54 \pm 0.52) \times 10^8$	$(3.13 \pm 0.62) \times 10^8$	$(5.03 \pm 2.43) \times 10^{16}$	8.1
EANA	$(6.66 \pm 0.62) \times 10^7$	$(1.83 \pm 0.49) \times 10^7$	$(1.24 \pm 0.45) \times 10^{15}$	1.1
Pya	$(2.20 \pm 0.56) \times 10^7$	$(5.24 \pm 0.56) \times 10^7$	$(1.14 \pm 0.25) \times 10^{15}$	9.5

[a] $K_{\text{total}} = K_1 \times K_2$. [b] Each data point is the average value of triplicate runs with the error being standard deviation. [c] Interaction factor $\alpha = 4K_2/K_1$. ($\alpha >$ 1: positive cooperativity; $\alpha <$ 1: negative cooperativity; $\alpha =$ 1 no cooperativity).

We also examined the cooperative interactions among the guest molecules, quantified by the interaction factor α ($\alpha = 4K_2/K_1$), where $\alpha > 1$ indicates positive cooperativity, $\alpha < 1$ indicates negative cooperativity, and $\alpha = 1$ suggests no cooperativity.[67,68] The α values for most of the guest molecules ranged from 1.1 to 15.8 (Table 1). Positive cooperativity observed for these guests implies that the binding of the first guest to the cavity of Naph-SAC4A facilitates the binding of the second guest, a phenomenon frequently observed in systems like γ-CD and CB[8]. This enhanced binding is likely due to additional π–π or dipole–dipole interactions between the two guest molecules, which promote cooperative encapsulation within the host cavity.

Across the 15 fluorescent dye guest molecules evaluated, despite their structural diversity, common features emerge: each possesses a hydrophobic aromatic conjugated framework, a planar, elongated molecular shape, and a positively charged pyridinium or ammonium group. These structural preferences align with Naph-SAC4A's recognition properties: its deep hydrophobic cavity drives guest encapsulation primarily through hydrophobic effects in aqueous solution, while the four aromatic walls facilitate π–π stacking with size-compatible aromatic polycyclic guests. Additionally, Naph-SAC4A's four negative charges enable electrostatic attraction with singly positively charged guests, enhancing affinity without inducing significant repulsion between the two encapsulated guests.

Molecular simulations and analysis

Due to the failure of all attempts to grow single crystals of ternary 1 : 2 host–guest complexes involving Naph-SAC4A under aqueous conditions, we resorted to computational simulations to elucidate how Naph-SAC4A binds to two guests.[69] It is important to note that computational simulations of host–guest complexes have inherent limitations, as the resulting conformations heavily rely on the initial configurations, which are inevitably biased. Here, we initially employed molecular

dynamics (MD) simulations to swiftly screen for potentially reasonable initial configurations, followed by density functional theory (DFT) calculations to obtain energy-minimized optimal conformations. Fig. 3 illustrates the optimized conformations of the Naph-SAC4A@2ADY-G and Naph-SAC4A@2ASP complexes obtained. Notably, owing to the conformational adaptability of Naph-SAC4A, two distinct binding modes are observed: two ADY-G molecules are arranged longitudinally along the cavity, while ASP is vertically oriented with respect to the four naphthyl azo fragments. Independent Gradient Model Based on Hirshfeld Partition (IGMH) analyses reveal multiple and diverse interactions between the host and guests, including [C–H···π], [π···π] stacking, and hydrogen bonds. Therefore, despite the notable limitations of computational simulations, they provide some valuable insights. At the very least, the optimized conformations demonstrate that the cavity of Naph-SC4A is sufficiently large to effectively encapsulate two ADY-G or ASP molecules, and also shed light on the potential 1 : 2 binding modes of Naph-SAC4A.

At a minimum, the optimized conformations confirm that Naph-SAC4A's cavity is spacious enough to encapsulate two ADY-G or ASP molecules, offering insights into potential 1 : 2 binding modes. Moreover, these conformations suggest that antiparallel stacking of the two guests may maximize separation of their positive charges, reducing electrostatic repulsion while enhancing favorable π–π stacking and dipole–dipole interactions. This arrangement supports a positive-cooperative binding process, consistent with our experimental observations.

Mass spectrometry analysis

High-resolution electrospray ionization mass spectrometry (HR-ESI-MS) was further employed due to its high sensitivity and precise mass accuracy for determining chemical binding stoichiometry.[70,71] Mass spectrometry data confirm the formation of
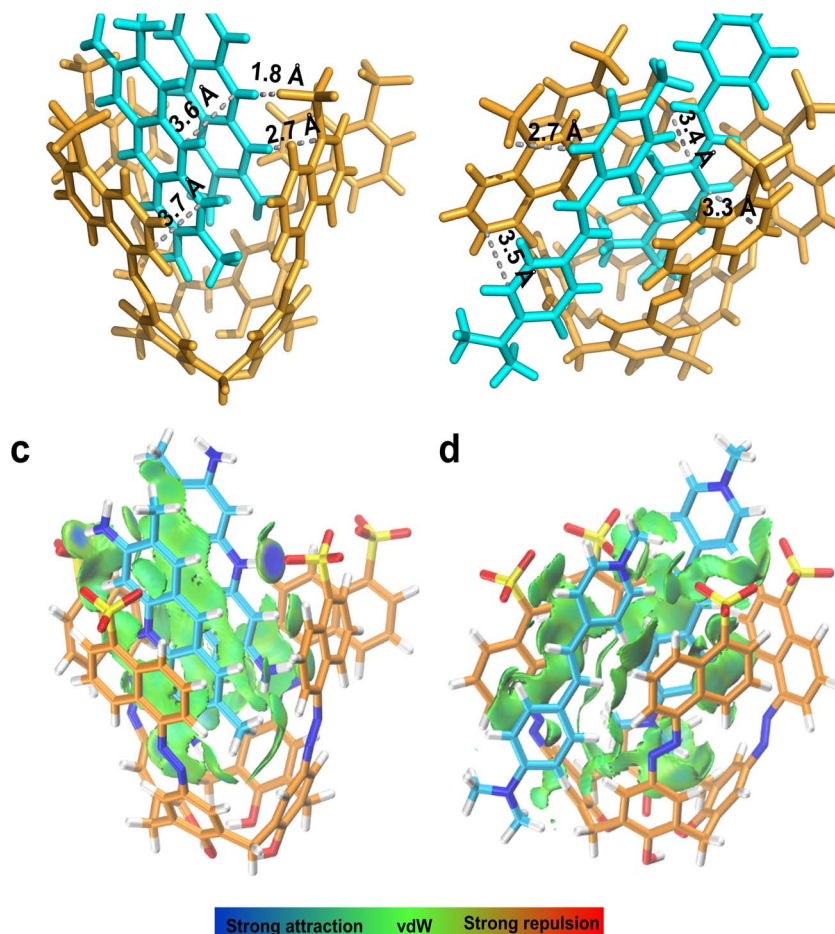
Fig. 3 Optimized binding geometry of the Naph-SAC4A@ADY-G (a) and Naph-SAC4A@ASP complex (b) at the B3LYP-D3/6-31G(d)/SMD(water) level of theory. δ_g^{inter} = 0.004 a.u. isosurfaces colored by the sign of $(\lambda_2)\rho$ for Naph-SAC4A@ADY-G (c) and Naph-SAC4A@ASP complex (d) (the meanings of δ_g^{inter} and sign $(\lambda_2)\rho$ are in ref. 67).

1 : 2 host–guest complexes in the gas phase but do not directly reflect the binding behavior in solution, which is influenced by factors such as molecular dynamics, solvent effects, and intermolecular interactions that are not observable by mass spectrometry. In this respect, four guest molecules (ASP, NR, Pya, and 6MNEP) were selected to form complexes with Naph-SAC4A in water and used in HR-ESI-MS measurements. As shown in Fig. S25† in the negative ion mode, the mass spectrometric peak for Naph-SAC4A appeared at m/z = 1359.1978, corresponding to the [Naph-SAC4A + 3H]$^-$ species. The relative molecular masses of the four dyes are as follows: ASP has a relative molecular mass of 294.41, NR has a relative molecular mass of 396.52, Pya has a relative molecular mass of 202.25, and 6MNEP has a relative molecular mass of 254.34. For the Naph-SAC4A and ASP mixed solution, two new peaks with relatively high intensities were observed at m/z = 798.16976 and 1835.49384, which correspond to the 1 : 1 complexing species, [Naph-SAC4A + ASP + H]$^{2-}$ and 1 : 2 complexing species, [Naph-SAC4A + 2ASP + H]$^-$, respectively. Similar analyses for the remaining three guest molecules binding to Naph-SAC4A revealed well-defined peaks of 1 : 2 complexing species at m/z = 1863.47485, 1821.40946, and 1909.46182, presenting [Naph-SAC4A + 2NR + H]$^-$, [Naph-

SAC4A + 2Pya + H]$^-$, and [Naph-SAC4A + 2(6MNEP) + H]$^-$, respectively. Meanwhile, 1 : 1 complexing peaks were also observed for the three guests. HR-ESI-MS analysis thus provides strong evidence for the formation of 1 : 2 host–guest complexes between Naph-SAC4A and the four guest dyes.

Preparation and characterization of a linear supramolecular polymer

The ability of Naph-SAC4A to form stable 1 : 2 ternary host–guest complexes with high affinity, coupled with its inherent hypoxia-responsiveness, makes it an ideal cleavable non-covalent connector. This unique characteristic positions Naph-SAC4A as a highly attractive component for the development of stimuli-responsive supramolecular polymeric materials. As a proof-of-concept, we synthesized a dimeric guest (D-Cy5) by linking two Cy5 derivatives *via* a hexaethylene glycol chain, which was used as a monomer for the preparation of linear supramolecular polymers. To improve the reproducibility and stability of the supramolecular polymer, we used a grinding method to ensure effective solid-state contact between components and avoid kinetic traps associated with direct aqueous mixing. In particular, D-Cy5 and Naph-SAC4A were ground

together in a 1 : 1 molar ratio to initiate supramolecular polymerization (Fig. 4a). The spontaneous formation of the linear supramolecular polymer resulted from the strong complexation between Naph-SAC4A and the Cy5 units. 2D diffusion ordered NMR spectroscopy (DOSY NMR) was then employed to investigate the polymerization process. The measured weighted average diffusion coefficients (D) considerably decreased from 3.327×10^{-10} to 5.156×10^{-11} m^2 s^{-1} as the concentration of the monomers increased from 0.50 to 5.0 mM (Fig. 4b). The approximately sevenfold reduction in D values with increasing concentration confirms the occurrence of concentration-dependent supramolecular polymerization.[72] Furthermore, analytical ultracentrifugation (AUC) analysis revealed that the average degree of polymerization (DP) of the supramolecular polymer increased from 30.4 ± 2.4 to 77.1 ± 3.0 as the monomer concentration increased from 5.0 to 40.0 μM (Fig. 4c). These results provide further evidence that the formation of a linear supramolecular polymer with relatively high molecular weights occurs in aqueous solution even at low concentrations owing to the high-affinity 1 : 2 complexation between Naph-SAC4A and Cy5.

The particle size of the supramolecular polymer was approximately 59.0 ± 6.5 nm at a concentration of 5.0 μM (Fig. 4d), as measured by dynamic light scattering (DLS). Transmission electron microscopy (TEM) images revealed spherical nanoparticles with a relatively uniform size of approximately around 51.2 ± 8.8 nm (Fig. 4d inset), consistent with the results of DLS measurements. Notably, when the concentration of the monomers was increased to 50.0 μM, the particle size increased to approximately 114.0 ± 7.8 nm, as measured by DLS (Fig. 4e), and the size of spherical nanoparticles increased to 106.0 ± 4.2 nm in the TEM image (Fig. 4e inset). The spherical morphology of the supramolecular polymer is ascribed to the self-aggregation of the linear supramolecular polymer chains in aqueous solution, which likely forms disordered, coil-like nanostructures. As the monomer's concentration increased, the degree of polymerization also increased, leading to the formation of larger spherical particles formed by self-aggregation of the supramolecular polymer with a higher degree of polymerization. This size increase further confirmed the occurrence of supramolecular polymerization and the correlation between particle size and monomer concentration.
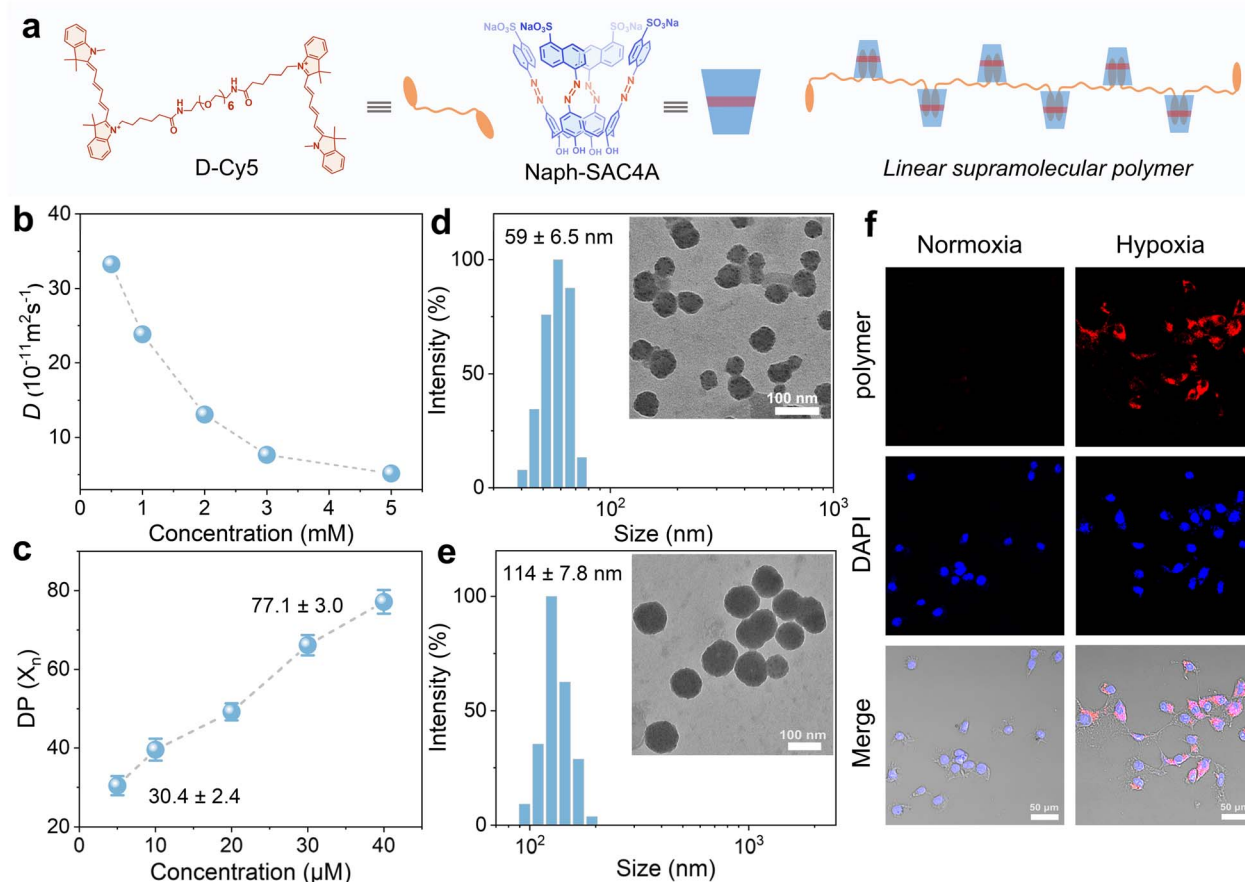

Fig. 4 (a) Schematic illustration of the formation of the Napth-SAC4A/D-Cy5 supramolecular polymer. (b) Concentration-dependent changes in diffusion coefficient values (D) of the Napth-SAC4A/D-Cy5 supramolecular polymer determined by DOSY NMR in D$_2$O. (c) Concentration-dependent changes in molecular weights of the supramolecular polymer determined by analytical ultracentrifugation (AUC) in PBS solution (10 mM, pH 7.4). The morphology and size of the supramolecular polymer at 5.0 μM (d) and 50 μM (e) were characterized by dynamic light scattering (DLS) and transmission electron microscopy (TEM). (f) Confocal laser scanning microscopy (CLSM) images of 4T1 cells incubated with the supramolecular polymer under hypoxic or normoxic conditions for 8 h. Scale bar: 50 μm. All data are expressed as means ± s.d.
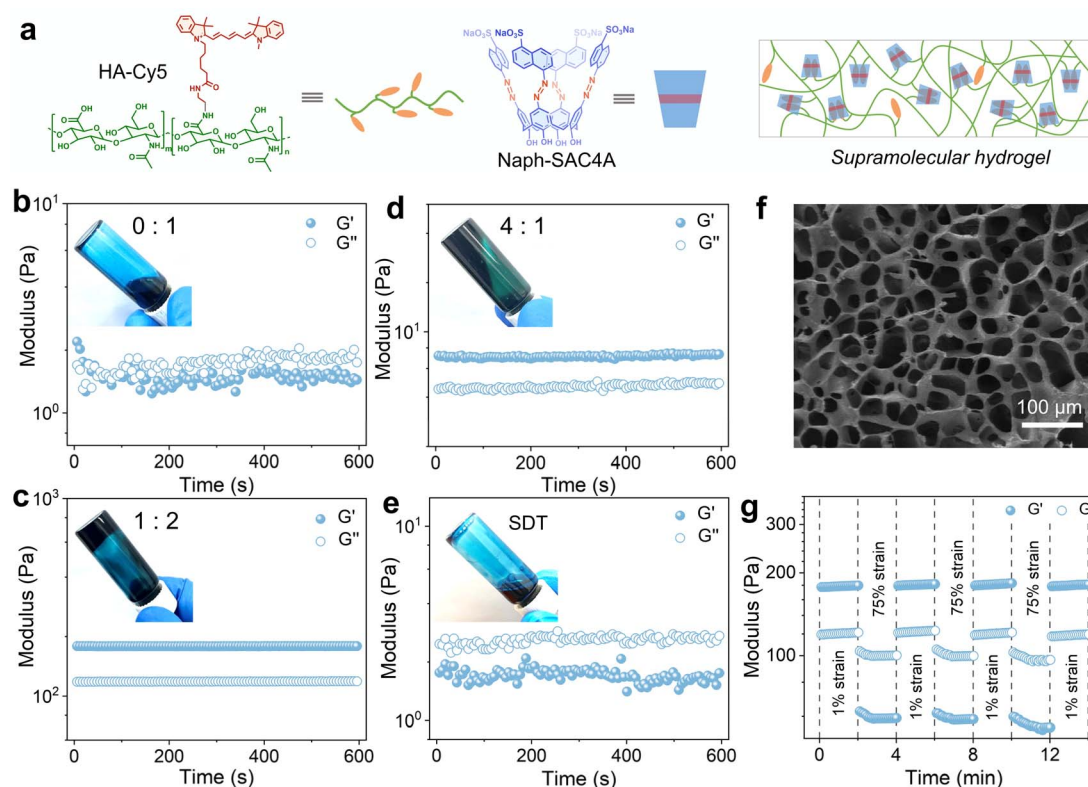
Fig. 5 (a) Schematic illustration of the formation of the Naph-SAC4A/HA-Cy5 hydrogel. (b) Time sweep rheological test of the Naph-SAC4A/HA-Cy5 hydrogel at a host−guest molar ratio of 0 : 1 (1% strain, 1 Hz, 0−600 s). (c) Time sweep rheological test of the Naph-SAC4A/HA-Cy5 hydrogel at a host−guest molar ratio of 1 : 2 (1% strain, 1 Hz, 0−600 s). (d) Time sweep rheological test of the Naph-SAC4A/HA-Cy5 hydrogel at a host−guest molar ratio of 4 : 1 (1% strain, 1 Hz, 0−600 s). (e) Time sweep rheological test of the Naph-SAC4A/HA-Cy5 hydrogel with the addition of SDT at a host−guest molar ratio of 1 : 2 (1% strain, 1 Hz, 0−600 s). (f) Microstructure of the Naph-SAC4A/HA-Cy5 hydrogel observed by scanning electron microscopy (SEM). (g) Time sweep rheological test of the Naph-SAC4A/HA-Cy5 hydrogel when alternated step strain was applied (the small strain was 1%, and the large strain was 75%).

Sodium dithionite (SDT) was added to the solution of Naph-SAC4A, respectively, and the absorbance at 420 nm was monitored continuously by UV-vis spectroscopy. Naph-SAC4A displayed broad absorption peaks above 400 nm, attributed to n–π^* transitions of the azo groups. Upon the addition of excess SDT, a chemical mimic of azo reductase, the absorption of the azo group at 420 nm significantly decreased (Fig. S27a†). Correspondingly, upon adding SDT to the solution of the supramolecular polymer, the fluorescence intensity of D-Cy5 was gradually restored over time, reaching saturation in 3 minutes (Fig. S27b†). After reduction, the host–guest binding ability of Naph-SAC4A was significantly diminished, releasing D-Cy5 from the cavities and gradually recovering the fluorescence signal.

Building on these results, we explored the potential of the supramolecular polymer for hypoxia-selective imaging in cells. As shown in Fig. 4f, when 4T1 cells were incubated with the supramolecular polymer (10.0 μM) under normoxic conditions, very low fluorescence signals were observed for the cells. In contrast, under hypoxic conditions, the cells exhibited much brighter fluorescence, demonstrating the hypoxia-responsive behavior.

Preparation and characterization of the supramolecular hydrogel

The strong 1 : 2 host–guest recognition of CB[8] has been widely exploited for the construction of supramolecular hydrogels.[73,74] Typically, responsive guest molecules, such as azobenzene[75,76] or spiropyran,[77–79] are incorporated into CB[8]-based hydrogels to introduce stimulus-responsiveness. In contrast, Naph-SAC4A, with its high affinity and hypoxia-responsiveness, enables the construction of responsive hydrogels with guest molecules that do not possess inherent stimulus-responsive properties. To verify the successful conjugation of Cy5 to hyaluronic acid (HA), we characterized the resulting HA-Cy5 conjugate using ^{1}H NMR and Fourier-transform infrared spectroscopy (FTIR). The results confirmed that Cy5 was successfully grafted onto HA (Fig. S7 and S29†). The grafting efficiency of Cy5 in the HA-Cy5 conjugate was determined to be 13.6% based on molar fraction, as calculated through UV-vis spectroscopy measurements (Fig. S28†). The supramolecular hydrogel was formed by mixing Naph-SAC4A and HA-Cy5 in aqueous solution driven by the 1 : 2 host–guest recognition between Naph-SAC4A and Cy5 (Fig. 5a). The dynamic mechanical properties of this supramolecular hydrogel were investigated by monitoring the storage modulus (G') and loss modulus (G'') over time at a strain

of 1% and a frequency of 1 Hz. In the absence of Naph-SAC4A, when only HA-Cy5 is present, the system remained in a sol state, with G'' consistently exceeding G' and exhibiting significant fluctuations (Fig. 5b). This behavior is attributed to the lack of sufficient entanglement between HA chains in the HA-Cy5 solution, due to the absence of cross-linking, preventing the formation of a stable hydrogel network. In contrast, when the host–guest molar ratio was set at 1 : 2, G' consistently exceeded G'', stabilizing at approximately 180 Pa and 118 Pa, respectively, which is characteristic of a typical hydrogel structure (Fig. 5c). The formation of ternary host–guest complexes between Naph-SAC4A and Cy5 provided robust noncovalent cross-linking points, enhancing the mechanical strength and stability of the hydrogel. However, when the host–guest molar ratio was increased to 4 : 1, G' remained greater than G'', but both moduli decreased to around 7 Pa and 4 Pa, respectively (Fig. 5d). This decrease in mechanical strength can be attributed to the partial conversion of ternary complexes into 1 : 1 binary complexes under conditions of excess host, leading to fewer cross-linking points between HA chains and, consequently, a reduction in the hydrogel's mechanical properties.

Subsequently, we investigated the microstructure and self-healing properties of the Naph-SAC4A/HA-Cy5 hydrogel. Scanning electron microscopy (SEM) imaging (Fig. 5f) revealed the presence of numerous micropores within the hydrogel, with an average pore size of approximately 65 μm. To assess the self-healing behavior, time sweep rheological tests were conducted, applying alternating strains of 1% and 75% to the hydrogel (Fig. 5g). Upon applying 75% strain, G'' rapidly increased, while G' sharply decreased from around 180 Pa to 60 Pa, indicating the disruption of the hydrogel's network structure. Once the applied strain was reduced to 1%, both G' and G'' quickly recovered to values near their initial levels. This cycle of destruction and recovery could be repeated multiple times, demonstrating that the Naph-SAC4A/HA-Cy5 hydrogel possesses excellent self-healing capabilities.

The addition of SDT to the hydrogel resulted in a significant change in the hydrogel's state from gel to sol (Fig. 5e). This shift is due to the reduction of Naph-SAC4A under hypoxic conditions, which leads to the loss of stable physical cross-linking points and a rapid decline in the mechanical strength of the hydrogel. Thus, the Naph-SAC4A/HA-Cy5 hydrogel demonstrates a hypoxia-responsive behavior, making it a promising candidate for stimuli-responsive supramolecular hydrogel applications.

Conclusion

Naph-SAC4A exhibits exceptional hypoxia-responsiveness alongside outstanding 1 : 2 binding affinities (ranging from 10^{14} to 10^{16} M^{-2}) with a variety of guest dyes. Its ability to form stable 1 : 2 host–guest complexes facilitates the modular construction of high-molecular-weight linear supramolecular polymers and self-healing supramolecular hydrogels, both of which demonstrate intelligent, hypoxia-responsive behavior. These features not only enhance the functionality of supramolecular materials but also open new avenues for designing dynamic, stimuli-

responsive systems with broad potential applications in drug delivery, tissue engineering, and diagnostic imaging. Additionally, the straightforward synthesis, high yield, and excellent water solubility of Naph-SAC4A significantly lower barriers to its use, making it highly accessible for a wider range of researchers and enabling its potential translation into real-world applications.

Data availability

The authors confirm that the data supporting the findings of this study are available within the article and as its ESI.†

Author contributions

S.-Y. Yao and A.-K. Ying performed materials synthesis, characterization, and manuscript preparation. W.-C. Geng, F.-Y. Chen, and X.-Y. Hu contributed to characterization. K. Cai and D.-S. Guo prepared the manuscript and supervised this work. All authors discussed experimental results.

Conflicts of interest

There are no conflicts to declare.

Acknowledgements

References

1 E. A. Meyer, R. K. Castellano and F. Diederich, Interactions with Aromatic Rings in Chemical and Biological Recognition, *Angew. Chem., Int. Ed.*, 2003, **42**(11), 1210–1250.

2 J. Li, J. X. Wang, H. X. Li, N. Song, D. Wang and B. Z. Tang, Supramol. Mater. based on AIE luminogens (AIEgens): construction and applications, *Chem. Soc. Rev.*, 2020, **49**(4), 1144–1172.

3 T. L. Mako, J. M. Racicot and M. Levine, Supramolecular Luminescent Sensors, *Chem. Rev.*, 2019, **119**(1), 322–477.

4 E. Mattia and S. Otto, Supramolecular systems chemistry, *Nat. Nanotechnol.*, 2015, **10**(2), 111–119.

5 R. Fu, D.-Y. Li, J.-H. Tian, Y.-L. Lin, Q.-Y. Zhao, W.-L. Li, F.-Y. Chen, D.-S. Guo and K. Cai, Enantiopure Corral[4] BINOLs as Ultrastrong Receptors for Recognition and Differential Sensing of Steroids, *Angew. Chem., Int. Ed.*, 2024, **63**(24), e202406233.

6 Z.-H. Wang, Y.-Q. Cheng, W.-B. Li, M.-M. Chen, S.-X. Zhang, Y.-C. Pan and D.-S. Guo, A Study of Chiral Biomedical Effects Based on Macrocyclic Carriers, *CCS Chem.*, 2024, DOI: **10.31635/ccschem.024.202404596**.

7 Y. Yuan, T. Nie, Y. Fang, X. You, H. Huang and J. Wu, Stimuli-responsive cyclodextrin-based supramolecular assemblies as drug carriers, *J. Mater. Chem. B*, 2022, **10**(13), 2077–2096.

8 H. Zhu, L. Chen, B. Sun, M. Wang, H. Li, J. F. Stoddart and F. Huang, Applications of macrocycle-based solid-state host-guest chemistry, *Nat. Rev. Chem*, 2023, **7**(11), 768–782.

9 N. Song, Z. Zhang, P. Liu, Y.-W. Yang, L. Wang, D. Wang and B. Z. Tang, Nanomaterials with Supramolecular Assembly Based on AIE Luminogens for Theranostic Applications, *Adv. Mater.*, 2020, **32**(49), 2004208.

10 J.-H. Tian, H. Xu, X.-Y. Hu and D.-S. Guo, Supramolecular fluorescence biosensing based on macrocycles, *Supramol. Mater.*, 2024, **3**, 100063.

11 D. Xia, P. Wang, X. Ji, N. M. Khashab, J. L. Sessler and F. Huang, Functional Supramolecular Polymeric Networks: The Marriage of Covalent Polymers and Macrocycle-Based Host-Guest Interactions, *Chem. Rev.*, 2020, **120**(13), 6070–6123.

12 Z. Yang, Y. Wang, X. Liu, R. T. Vanderlinden, R. Ni, X. Li and P. J. Stang, Hierarchical Self-Assembly of a Pyrene-Based Discrete Organoplatinum(II) Double-Metallacycle with Triflate Anions via Hydrogen Bonding and Its Tunable Fluorescence Emission, *J. Am. Chem. Soc.*, 2020, **142**(32), 13689–13694.

13 T. Sahu, Y. K. Ratre, S. Chauhan, L. Bhaskar, M. P. Nair and H. K. Verma, Nanotechnology based drug delivery system: Current strategies and emerging therapeutic potential for medical science, *J. Drug Delivery Sci. Technol.*, 2021, **63**, 102487.

14 Y. Liang, E. Li, K. Wang, Z.-J. Guan, H.-h. He, L. Zhang, H.-C. Zhou, F. Huang and Y. Fang, Organo-macrocycle-containing hierarchical metal-organic frameworks and cages: design, structures, and applications, *Chem. Soc. Rev.*, 2022, **51**(19), 8378–8405.

15 C. Zhang, A.-F. Liu, S. Li, F.-Y. Chen, J.-T. Zhang, F.-X. Zeng, H.-C. Feng, P. Wang, W.-C. Geng, C.-R. Ma and D.-S. Guo, A supramolecular formulation of icariin@sulfonatoazocalixarene for hypoxia-targeted osteoarthritis therapy, *Chin. Chem. Lett.*, 2025, **36**(1), 109752.

16 S. J. Barrow, S. Kasera, M. J. Rowland, J. del Barrio and O. A. Scherman, Cucurbituril-Based Molecular Recognition, *Chem. Rev.*, 2015, **115**(22), 12320–12406.

17 D.-S. Guo and Y. Liu, Supramolecular Chemistry of p-Sulfonatocalix[n]arenes and Its Biological Applications, *Acc. Chem. Res.*, 2014, **47**(7), 1925–1934.

18 S. Kundu, T. K. Egboluche and M. A. Hossain, Urea- and Thiourea-Based Receptors for Anion Binding, *Acc. Chem. Res.*, 2023, **56**(11), 1320–1329.

19 R. Fu, Q.-Y. Zhao, H. Han, W.-L. Li, F.-Y. Chen, C. Tang, W. Zhang, S.-D. Guo, D.-Y. Li, W.-C. Geng, D.-S. Guo and K. Cai, A Chiral Emissive Conjugated Corral for High-Affinity and Highly Enantioselective Recognition in Water, *Angew. Chem., Int. Ed.*, 2023, **62**(51), e202315990.

20 J.-R. Wu, D. Li, G. Wu, M.-H. Li and Y.-W. Yang, Modulating Supramolecular Charge-Transfer Interactions in the Solid State using Compressible Macrocyclic Hosts, *Angew. Chem., Int. Ed.*, 2022, **61**(43), e202210579.

21 T. Ogoshi, T.-a. Yamagishi and Y. Nakamoto, Pillar-Shaped Macrocyclic Hosts Pillar[n]arenes: New Key Players for Supramolecular Chemistry, *Chem. Rev.*, 2016, **116**(14), 7937–8002.

22 J.-C. Gui, Z.-Q. Yan, Y. Peng, J.-G. Yi, D.-Y. Zhou, D. Su, Z.-H. Zhong, G.-W. Gao, W.-H. Wu and C. Yang, Enhanced head-to-head photodimers in the photocyclodimerization of anthracenecarboxylic acid with a cationic pillar[6]arene, *Chin. Chem. Lett.*, 2016, **27**(7), 1017–1021.

23 Q. Wang, Y. Zhong, D. P. Miller, X. Lu, Q. Tang, Z.-L. Lu, E. Zurek, R. Liu and B. Gong, Self-Assembly and Molecular Recognition in Water: Tubular Stacking and Guest-Templated Discrete Assembly of Water-Soluble, Shape-Persistent Macrocycles, *J. Am. Chem. Soc.*, 2020, **142**(6), 2915–2924.

24 S. Yang, D. Larsen, M. Pellegrini, S. Meier, D. F. Mierke, S. R. Beeren and I. Aprahamian, Dynamic enzymatic synthesis of γ-cyclodextrin using a photoremovable hydrazone template, *Chem*, 2021, **7**(8), 2190–2200.

25 X. Yang, B. Yang, Y. Deng, X. Xie, Y. Qi, G. Yan, X. Peng, P. Zhao and L. Bian, Coacervation-Mediated Cytocompatible Formation of Supramolecular Hydrogels with Self-Evolving Macropores for 3D Multicellular Spheroid Culture, *Adv. Mater.*, 2023, **35**(24), 2300636.

26 A. Harada, J. Li and M. Kamachi, Double-stranded inclusion complexes of cyclodextrin threaded on poly(ethylene glycol), *Nature*, 1994, **370**(6485), 126–128.

27 M. Raeisi, K. Kotturi, I. del Valle, J. Schulz, P. Dornblut and E. Masson, Sequence-Specific Self-Assembly of Positive and Negative Monomers with Cucurbit[8]uril Linkers, *J. Am. Chem. Soc.*, 2018, **140**(9), 3371–3377.

28 W. Han, W. Xiang, Q. Li, H. Zhang, Y. Yang, J. Shi, Y. Ji, S. Wang, X. Ji, N. M. Khashab and J. L. Sessler, Water compatible supramolecular polymers: recent progress, *Chem. Soc. Rev.*, 2021, **50**(18), 10025–10043.

29 K. I. Assaf and W. M. Nau, Cucurbiturils: from synthesis to high-affinity binding and catalysis, *Chem. Soc. Rev.*, 2015, **44**(2), 394–418.

30 J. Yu, W. Ha, J.-n. Sun and Y.-p. Shi, Supramolecular Hybrid Hydrogel Based on Host–Guest Interaction and Its Application in Drug Delivery, *ACS Appl. Mater. Interfaces*, 2014, **6**(22), 19544–19551.

31 E. A. Appel, F. Biedermann, U. Rauwald, S. T. Jones, J. M. Zayed and O. A. Scherman, Supramolecular Cross-Linked Networks via Host-Guest Complexation with Cucurbit[8]uril, *J. Am. Chem. Soc.*, 2010, **132**(40), 14251–14260.

32 J. Krämer, L. M. Grimm, C. Zhong, M. Hirtz and F. Biedermann, A supramolecular cucurbit[8]uril-based rotaxane chemosensor for the optical tryptophan detection in human serum and urine, *Nat. Commun.*, 2023, **14**(1), 518.

33 Z. X. Liu and Y. Liu, Multicharged cyclodextrin supramolecular assemblies, *Chem. Soc. Rev.*, 2022, **51**(11), 4786–4827.

34 H. Han, R. Fu, R. Wang, C. Tang, M.-M. He, J.-Y. Deng, D.-S. Guo, J. F. Stoddart and K. Cai, Corralarenes: A Family

of Conjugated Tubular Hosts, *J. Am. Chem. Soc.*, 2022, **144**(44), 20351–20362.

35 C. Tu, W. Wu, W. Liang, D. Zhang, W. Xu, S. Wan, W. Lu and C. Yang, Host-Guest Complexation-Induced Aggregation Based on Pyrene-Modified Cyclodextrins for Improved Electronic Circular Dichroism and Circularly Polarized Luminescence, *Angew. Chem., Int. Ed.*, 2022, **61**(29), e202203541.

36 S. Sonzini, A. Marcozzi, R. J. Gubeli, C. F. vander Walle, P. Ravn, A. Herrmann and O. A. Scherman, High Affinity Recognition of a Selected Amino Acid Epitope within a Protein by Cucurbit[8]uril Complexation, *Angew. Chem., Int. Ed.*, 2016, **55**(45), 14000–14004.

37 K. Liu, Y. Jiang, Z. Bao and X. Yan, Skin-Inspired Electronics Enabled by Supramolecular Polymeric Materials, *CCS Chem.*, 2019, **1**(4), 431–447.

38 J. d. Barrio, J. Liu, R. A. Brady, C. S. Y. Tan, S. Chiodini, M. Ricci, R. Fernández-Leiro, C.-J. Tsai, P. Vasileiadi, L. Di Michele, D. Lairez, C. Toprakcioglu and O. A. Scherman, Emerging Two-Dimensional Crystallization of Cucurbit[8] uril Complexes: From Supramolecular Polymers to Nanofibers, *J. Am. Chem. Soc.*, 2019, **141**(36), 14021–14025.

39 J. Yao, Z. Yan, J. Ji, W. Wu, C. Yang, M. Nishijima, G. Fukuhara, T. Mori and Y. Inoue, Ammonia-driven chirality inversion and enhancement in enantiodifferentiating photocyclodimerization of 2-anthracenecarboxylate mediated by diguanidino-γ-cyclodextrin, *J. Am. Chem. Soc.*, 2014, **136**(19), 6916–6919.

40 S. Y. Jon, N. Selvapalam, D. H. Oh, J.-K. Kang, S.-Y. Kim, Y. J. Jeon, J. W. Lee and K. Kim, Facile Synthesis of Cucurbit[n]uril Derivatives via Direct Functionalization: Expanding Utilization of Cucurbit[n]uril, *J. Am. Chem. Soc.*, 2003, **125**(34), 10186–10187.

41 J.-X. Liu, K. Chen and C. Redshaw, Stimuli-responsive mechanically interlocked molecules constructed from cucurbit[n]uril homologues and derivatives, *Chem. Soc. Rev.*, 2023, **52**(4), 1428–1455.

42 Y. J. Jeon, H. Kim, S. Jon, N. Selvapalam, D. H. Oh, I. Seo, C.-S. Park, S. R. Jung, D.-S. Koh and K. Kim, Artificial Ion Channel Formed by Cucurbit[n]uril Derivatives with a Carbonyl Group Fringed Portal Reminiscent of the Selectivity Filter of K$^+$ Channels, *J. Am. Chem. Soc.*, 2004, **126**(49), 15944–15945.

43 Y. Jiao, Y. Qiu, L. Zhang, W.-G. Liu, H. Mao, H. Chen, Y. Feng, K. Cai, D. Shen, B. Song, X.-Y. Chen, X. Li, X. Zhao, R. M. Young, C. L. Stern, M. R. Wasielewski, R. D. Astumian, W. A. Goddard and J. F. Stoddart, Electron-catalysed molecular recognition, *Nature*, 2022, **603**(7900), 265–270.

44 E. A. Appel, X. J. Loh, S. T. Jones, F. Biedermann, C. A. Dreiss and O. A. Scherman, Ultrahigh-Water-Content Supramolecular Hydrogels Exhibiting Multistimuli Responsiveness, *J. Am. Chem. Soc.*, 2012, **134**(28), 11767–11773.

45 L. Barravecchia, A. Blanco-Gómez, I. Neira, R. Skackauskaite, A. Vila, A. Rey-Rico, C. Peinador and M. D. García, "Vermellogens" and the Development of CB[8]-Based

Supramolecular Switches Using pH-Responsive and Non-Toxic Viologen Analogues, *J. Am. Chem. Soc.*, 2022, **144**(41), 19127–19136.

46 F.-Y. Chen, C.-Z. Li, H. Han, W.-C. Geng, S.-X. Zhang, Z.-T. Jiang, Q.-Y. Zhao, K. Cai and D.-S. Guo, Expanding the Hydrophobic Cavity Surface of Azocalix[4]arene to Enable Biotin/Avidin Affinity with Controlled Release, *Angew. Chem., Int. Ed.*, 2024, **63**(23), e202402139.

47 Y.-C. Pan, X.-Y. Hu and D.-S. Guo, Biomedical Applications of Calixarenes: State of the Art and Perspectives, *Angew. Chem., Int. Ed.*, 2021, **60**(6), 2768–2794.

48 F.-Y. Chen, W.-C. Geng, K. Cai and D.-S. Guo, Molecular recognition of cyclophanes in water, *Chin. Chem. Lett.*, 2024, **35**(5), 109161.

49 X.-Y. Hu, R. Fu and D.-S. Guo, Hypoxia-Responsive Host-Guest Drug Delivery System, *Acc. Mater. Res.*, 2023, **4**(11), 925–938.

50 W.-C. Geng, S. Jia, Z. Zheng, Z. Li, D. Ding and D.-S. Guo, A Noncovalent Fluorescence Turn-on Strategy for Hypoxia Imaging, *Angew. Chem., Int. Ed.*, 2019, **58**(8), 2377–2381.

51 A. Sharma, J. F. Arambula, S. Koo, R. Kumar, H. Singh, J. L. Sessler and J. S. Kim, Hypoxia-targeted drug delivery, *Chem. Soc. Rev.*, 2019, **48**(3), 771–813.

52 Y.-C. Pan, J.-H. Tian and D.-S. Guo, Molecular Recognition with Macrocyclic Receptors for Application in Precision Medicine, *Acc. Chem. Res.*, 2023, **56**(24), 3626–3639.

53 L.-P. Yang, X. Wang, H. Yao and W. Jiang, Naphthotubes: Macrocyclic Hosts with a Biomimetic Cavity Feature, *Acc. Chem. Res.*, 2020, **53**(1), 198–208.

54 S. Li, R. Ma, X.-Y. Hu, H.-B. Li, W.-C. Geng, X. Kong, C. Zhang and D.-S. Guo, Drug in Drug: A Host-Guest Formulation of Azocalixarene with Hydroxychloroquine for Synergistic Anti-Inflammation, *Adv. Mater.*, 2022, **34**(32), 2203765.

55 J.-J. Li, Y. Hu, B. Hu, W. Wang, H. Xu, X.-Y. Hu, F. Ding, H.-B. Li, K.-R. Wang, X. Zhang and D.-S. Guo, Lactose azocalixarene drug delivery system for the treatment of multidrug-resistant pseudomonas aeruginosa infected diabetic ulcer, *Nat. Commun.*, 2022, **13**(1), 6279.

56 F.-Y. Chen, W.-C. Geng, K. Cai and D.-S. Guo, Molecular recognition of cyclophanes in water, *Chin. Chem. Lett.*, 2024, **35**(5), 109161.

57 H.-B. Cheng, S. Zhang, J. Qi, X.-J. Liang and J. Yoon, Advances in Application of Azobenzene as a Trigger in Biomedicine: Molecular Design and Spontaneous Assembly, *Adv. Mater.*, 2021, **33**(26), 2007290.

58 X.-L. Ni, S. Chen, Y. Yang and Z. Tao, Facile Cucurbit[8]uril-Based Supramolecular Approach To Fabricate Tunable Luminescent Materials in Aqueous Solution, *J. Am. Chem. Soc.*, 2016, **138**(19), 6177–6183.

59 C. D. Gutsche and L.-G. Lin, Calixarenes 12: The synthesis of functionalized calixarenes, *Tetrahedron*, 1986, **42**(6), 1633–1640.

60 Y.-X. Yue, Y.-L. Lin, M.-M. Chen, H.-W. Tian, R. Ma, Z.-H. Wang, F.-Y. Chen, Y.-C. Pan and D.-S. Guo, Azocalixarenes: a scaffold of universal excipients with high efficiency, *Sci. China:Chem.*, 2024, **67**(5), 1697–1706.

61 M. Yamashina, S. Kusaba, M. Akita, T. Kikuchi and M. Yoshizawa, Cramming versus threading of long amphiphilic oligomers into a polyaromatic capsule, *Nat. Commun.*, 2018, **9**(1), 4227.

62 D. J. Cram and J. M. Cram, Host-Guest Chemistry, *Science*, 1974, **183**(4127), 803–809.

63 W. C. Geng, Z. Zheng and D. S. Guo, Supramolecular design based activatable magnetic resonance imaging, *View*, 2021, **2**(2), 20200059.

64 Y.-X. Yue, Z. Zhang, Z.-H. Wang, R. Ma, M.-M. Chen, F. Ding, H.-B. Li, J.-J. Li, L. Shi, Y. Liu and D.-S. Guo, Promoting Tumor Accumulation of Anticancer Drugs by Hierarchical Carrying of Exogenous and Endogenous Vehicles, *Small Struct.*, 2022, **3**(10), 2200067.

65 J.-S. Guo, J.-J. Li, Z.-H. Wang, Y. Liu, Y.-X. Yue, H.-B. Li, X.-H. Zhao, Y.-J. Sun, Y.-H. Ding, F. Ding, D.-S. Guo, L. Wang and Y. Chen, Dual hypoxia-responsive supramolecular complex for cancer target therapy, *Nat. Commun.*, 2023, **14**(1), 5634.

66 E. Merino, Synthesis of azobenzenes: the coloured pieces of molecular materials, *Chem. Soc. Rev.*, 2011, **40**(7), 3835–3853.

67 As highlighted in the literature (Thordarson P., Determining association constants from titration experiments in supramolecular chemistry. Chem. Soc. Rev., 2011, **40**, 3, 1305–1323), the Job plot method has certain limitations in determining binding stoichiometry. Specifically, for complex 1:2 binding systems, it may yield misleading results. The observed maxima in the Job plot can deviate from the ideal value of 0.66 under conditions such as weak binding, low concentrations, or large discrepancies between K_1 and K_2. However, in this study, the generally high binding affinities of Naph-SAC4A with the guests, coupled with the similar magnitudes of K_1 and K_2, result in a well-defined inflection point in the Job plot, thereby confirming the 1:2 binding mode. Additionally, the findings were rigorously validated through repeated experiments, fitting analysis, and HR-ESI-MS measurements.

68 D. Brynn Hibbert and P. Thordarson, The death of the Job plot, transparency, open science and online tools, uncertainty estimation methods and other developments in supramolecular chemistry data analysis, *Chem. Commun.*, 2016, **52**(87), 12792–12805.

69 X. Cheng, R. Chen, J. E. Bruce, B. L. Schwartz, G. A. Anderson, S. A. Hofstadler, D. C. Gale, R. D. Smith, J. Gao, G. B. Sigal, M. Mammen and G. M. Whitesides, Using Electrospray Ionization FTICR Mass Spectrometry To Study Competitive Binding of Inhibitors to Carbonic Anhydrase, *J. Am. Chem. Soc.*, 1995, **117**(34), 8859–8860.

70 K. X. Wan, T. Shibue and M. L. Gross, Non-Covalent Complexes between DNA-Binding Drugs and Double-Stranded Oligodeoxynucleotides: A Study by ESI Ion-Trap Mass Spectrometry, *J. Am. Chem. Soc.*, 2000, **122**(2), 300–307.

71 Y.-K. Tian, Y.-G. Shi, Z.-S. Yang and F. Wang, Responsive Supramolecular Polymers Based on the Bis[alkynylplatinum(II)] Terpyridine Molecular Tweezer/Arene Recognition Motif, *Angew. Chem., Int. Ed.*, 2014, **53**(24), 6090–6094.

72 C. S. Y. Tan, J. Liu, A. S. Groombridge, S. J. Barrow, C. A. Dreiss and O. A. Scherman, Controlling Spatiotemporal Mechanics of Supramolecular Hydrogel Networks with Highly Branched Cucurbit[8]uril Polyrotaxanes, *Adv. Funct. Mater.*, 2018, **28**(7), 1702994.

73 Y. Wang, A. M. Bimmermann, M. Neufurth and P. Besenius, Cucurbit[8]uril Mediated Supramolecular and Photocrosslinked Interpenetrating Network Hydrogel Matrices for 3D-Bioprinting, *Adv. Mater.*, 2024, **36**(26), 2313270.

74 J.-H. Hu, Y. Huang, C. Redshaw, Z. Tao and X. Xiao, Cucurbit[n]uril-based supramolecular hydrogels: Synthesis, properties and applications, *Coord. Chem. Rev.*, 2023, **489**, 215194.

75 H. Wang, C. N. Zhu, H. Zeng, X. Ji, T. Xie, X. Yan, Z. L. Wu and F. Huang, Reversible Ion-Conducting Switch in a Novel Single-Ion Supramolecular Hydrogel Enabled by Photoresponsive Host-Guest Molecular Recognition, *Adv. Mater.*, 2019, **31**(12), 1807328.

76 Y. Li, B. Xue, J. Yang, J. Jiang, J. Liu, Y. Zhou, J. Zhang, M. Wu, Y. Yuan, Z. Zhu, Z. J. Wang, Y. Chen, Y. Harabuchi, T. Nakajima, W. Wang, S. Maeda, J. P. Gong and Y. Cao, Azobenzene as a photoswitchable mechanophore, *Nat. Chem.*, 2024, **16**(3), 446–455.

77 C. Li, A. Iscen, L. C. Palmer, G. C. Schatz and S. I. Stupp, Light-Driven Expansion of Spiropyran Hydrogels, *J. Am. Chem. Soc.*, 2020, **142**(18), 8447–8453.

78 M. Du and C. Li, Engineering Supramolecular Hydrogels via Reversible Photoswitching of Cucurbit[8]uril-Spiropyran Complexation Stoichiometry, *Adv. Mater.*, 2024, **36**(40), 2408484.

79 C. Li, Y. Xue, M. Han, L. C. Palmer, J. A. Rogers, Y. Huang and S. I. Stupp, Synergistic photoactuation of bilayered spiropyran hydrogels for predictable origami-like shape change, *Matter*, 2021, **4**(4), 1377–1390.